minerals

MDPI

Article

Fluorluanshiweiite, $KLiAl_{1.5}\square_{0.5}(Si_{3.5}Al_{0.5})O_{10}F_2$, a New Mineral of the Mica Group from the Nanyangshan LCT Pegmatite Deposit, North Qinling Orogen, China

Kai Qu [1,*], Xianzhang Sima [1], Guowu Li [2], Guang Fan [3], Ganfu Shen [4], Xing Liu [1], Zhibin Xiao [1], Hu Guo [1], Linfei Qiu [3] and Yanjuan Wang [2]

1 Tianjin Center, China Geological Survey, Tianjin 300170, China; smxz_tcgs@foxmail.com (X.S.); liuxing_tcgs@163.com (X.L.); zhibin_xiao@163.com (Z.X.); 028huguo@163.com (H.G.)
2 Crystal Structure Laboratory, China University of Geosciences (Beijing), Beijing 100083, China; liguowu@cugb.edu.cn (G.L.); wangyanjuan_cugb@foxmail.com (Y.W.)
3 Beijing Research Institute of Uranium Geology, Beijing 100029, China; fanguang2008@163.com (G.F.); qlf0602@163.com (L.Q.)
4 Chengdu Center, China Geological Survey, Chengdu 610081, China; sgf829@126.com
* Correspondence: qukai_tcgs@foxmail.com; Tel.: +86-022-8411-2984

Received: 3 December 2019; Accepted: 18 January 2020; Published: 21 January 2020

Abstract: A new mineral species of the mica group, fluorluanshiweiite, ideally $KLiAl_{1.5}\square_{0.5}(Si_{3.5}Al_{0.5})O_{10}F_2$, has been found in the Nanyangshan LCT (Li, Cs, Ta) pegmatite deposit in North Qinling Orogen (NQO), central China. Fluorluanshiweiite can be regarded as the F-dominant analogue at the *A* site of luanshiweiite or the K-dominant analogue at the *I* site of voloshinite. It appears mostly in cookeite as a flaky residue, replaced by Cs-rich mica, or in the form of scale aggregates. Most individual grains are <1 mm in size, with the largest being ca. 1 cm, and the periphery is replaced by cookeite. No twinning is observed. The mineral is silvery white as a hand specimen, and in a thin section, it appears grayish-white to colorless, transparent with white streaks, with vitreous luster and pearliness on cleavage faces. It is flexible with micaceous fracture; the Mohs hardness is approximately 3; the cleavage is perfect on {001}; and no parting is observed. The measured and calculated densities are 2.94(3) and 2.898 g/cm^3, respectively. Optically, fluorluanshiweiite is biaxial (–), with $\alpha = 1.554(1)$, $\beta = 1.581(1)$, $\gamma = 1.583(1)$ (white light), $2V$(meas.) = 25° to 35°, $2V$(calc.) = 30.05°. The calculated compatibility index based on the empirical formula is −0.014 (superior). An electron microprobe analysis yields the empirical formula calculated based on 10 O atoms and 2 additional anions of $(K_{0.85}Rb_{0.12}Cs_{0.02}Na_{0.03})_{\Sigma 1.02}[Li_{1.05}Al_{1.44}(\square_{0.47}Fe_{0.01}Mn_{0.02})_{\Sigma 0.5}]_{\Sigma 2.99}(Si_{3.55}Al_{0.45})_{\Sigma 4}O_{10}F_2$, which can be simplified to $KLiAl_{1.5}\square_{0.5}(Si_{3.5}Al_{0.5})O_{10}F_2$. Fluorluanshiweiite is monoclinic with the space group *C*2/*m* and unit cell parameters $a = 5.2030(5)$, $b = 8.9894(6)$, $c = 10.1253(9)$ Å, $\beta = 100.68(1)°$, and $V = 465.37(7)$ Å^3. The strongest eight lines in the X-ray diffraction data are [*d* in Å(*I*)(hkl)]: 8.427(25) (001), 4.519(57) (020), 4.121(25) (021), 3.628(61) ($\bar{1}$12), 3.350(60) (022), 3.091(46) (112), 2.586(100) ($\bar{1}$30), and 1.506(45) (312).

Keywords: fluorluanshiweiite; mica group; new mineral species; chemical composition; crystal structure; North Qinling Orogen; China

1. Introduction

A new mineral species of the mica group, $KLiAl_{1.5}\square_{0.5}(Si_{3.5}Al_{0.5})O_{10}F_2$, has been found in the Nanyangshan LCT pegmatite deposit in North Qinling Orogen (NQO), Central China (33°52′58″ N,

110°43′55″ E). It is named fluorluanshiweiite based on its relationship to luanshiweiite. It is characterized as F-dominant at the *A* site of luanshiweiite [1] or K-dominant at the *I* site of voloshinite [2]. The new mineral (IMA2019-053) has been approved by the Commission on New Minerals, Nomenclature and Classification of the International Mineralogical Association (IMA-CNMNC) [3]. The material was deposited in the mineralogical collection of the Geological Museum of China, No. 16, Xisi Yangrou Hutong, Xicheng District, Beijing 100034, People's Republic of China (catalogue number: M16085). This paper describes the physical, chemical, and spectroscopic data of fluorluanshiweiite and its crystal structure.

2. Occurrence and Physical Properties

The Nanyangshan rare metal deposit is located in NQO, Western Henan Province, central China. The rare metal mineralization is hosted in granitic pegmatite [4]. According to the classification and revision by Černý [5] and Černý and Ercit [6], it is classified as LCT pegmatite. The Ar-Ar dating of muscovite revealed that the Nanyangshan pegmatite formed at 396–410 Ma [7], and the age coincides with the time of U-REE-rare metal mineralization (mean = 408 Ma) in NQO [8–10], shortly after 400–428 Ma (mean = 417 Ma), when the related intrusions formed, indicating that the mineral formed in the late stage of the evolution of a pegmatite-forming magmatic liquid. The new mineral is closely associated with luanshiweiite (first recorded locality [1]), polylithionite, cookeite, albite, quartz and an unknown Cs-rich mica (Figure 1a,b), and it is commonly found with spodumene, montebrasite, elbaite, fluorapatite, pollucite, and nanpingite. Tantalite-(Mn), columbite-(Mn), bismutotantalite, stibiotantalite, oxynatromicrolite (first recorded locality [11]), and fluornatromicrolite are some other associated minerals.

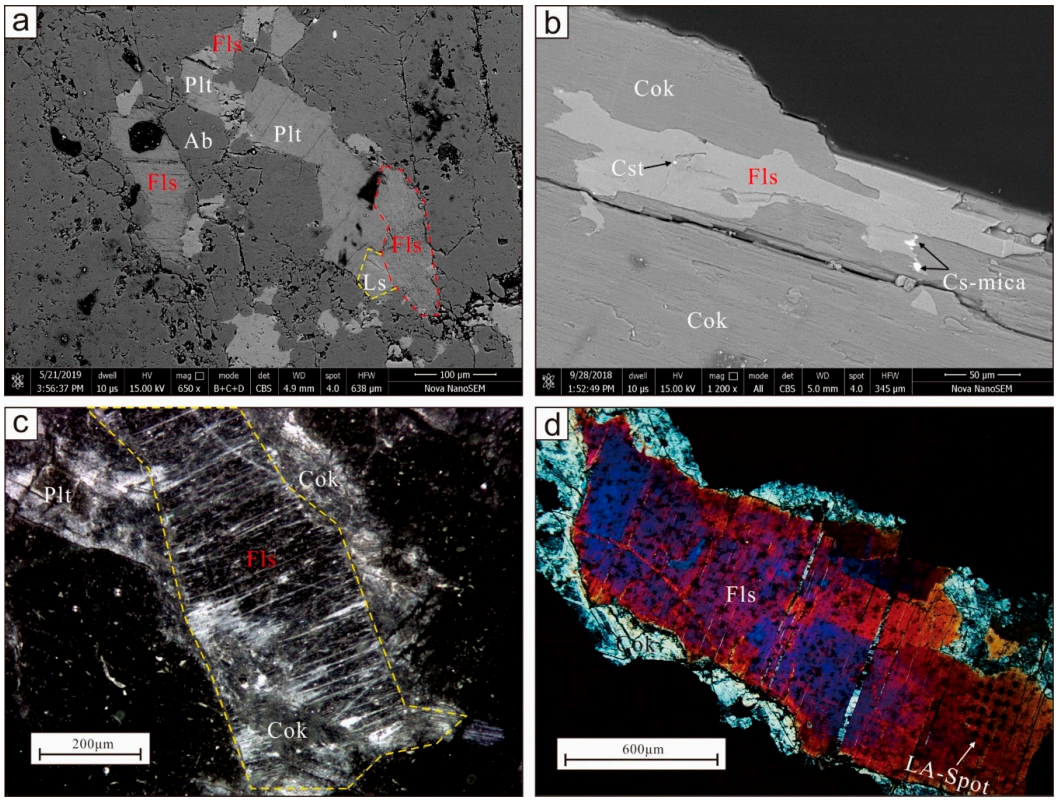

Figure 1. (**a**) and (**b**) Backscattered electron images of mineral aggregates; (**c**) fluorluanshiweiite under binocular microscope; (**d**) grains for single-crystal X-ray analysis under cross-polarized light. Fls, fluorluanshiweiite; Ls, luanshiweiite; Plt, polylithionite; Cok, cookeite; Cst, cassiterite; Ab, Albite.

Fluorluanshiweiite occurs mostly in cookeite as a flaky residue, replaced by Cs-rich mica, or n the form of scale aggregates. Most individual grains are <1 mm in size, with the largest being ca. 1 cm, and the periphery is replaced by cookeite (Figure 1c,d). The mineral is silvery white as a hand specimen and grayish-white to colorless in a thin section, transparent with white streaks. In addition, it has vitreous luster and appears pearly on cleavage planes. It is flexible with micaceous fracture, the Mohs hardness is approximately 3, the cleavage is perfect on {001}, and no parting was observed. The measured and calculated densities are 2.94(3) and 2.898 g/cm^3, respectively. Optically, fluorluanshiweiite is biaxial (–) with α = 1.554(1), β = 1.581(1), γ = 1.583(1) (white light), 2*V* (meas.) = 25° to 35°, 2*V* (calc.) = 30.05°. The calculated compatibility (1-K_P/K_C) is superior (−0.014) [12].

3. Chemical Composition

The chemical compositions of the fluorluanshiweiite and associated luanshiweiite and polylithionite were determined at the Beijing Research Institute of Uranium Geology with a JXA-8100 electron microprobe at 15 kV and 10 nA with a beam diameter of 10 μm. The F*Kα* was determined with an LDE1 crystal (JEOL, 2d ≈ 6 nm), which is suitable for the analysis of ^{6}C–^{10}Ne, and the P/B ratio is much higher than that of the TAP crystal for F. The standards include phlogopite for K, Fe and Al; pollucite for Rb and Cs; albite for Na; tantalite-(Mn) for Mn; sanidine for Si and fluorapatite for F. The fluorine migration and peak overlap have been fully considered in the factors affecting the accurate quantification of F in the EPMA process to ensure that the results are reliable. The lithium content analysis was carried out using an LA-MC-ICP-MS instrument (Neptune, Thermo Fisher Scientific) equipped with a (ESI) NewWare 193 FX ArF Excimer laser ablation system with a 193-nm wavelength. The operating conditions were as follows: beam diameter = 30 μm, alongside a laser pulse rate of 8 Hz with an energy density of approximately 4 J/cm^2; N = 20. The obtained results were consistent with the data (3.95% Li_2O) determined by atomic absorption spectroscopy (AAS). Scanning electron microscopy investigations were performed with an FEI Nova Nano scanning electron microscope (SEM) (10 μs; 15 kV). The anhydrous nature of the studied mineral was indicated by the absence of OH stretching vibration absorption in the ATR-FT/IR spectrum, as shown below.

Twenty electron microprobe point analyses for fluorluanshiweiite yielded an average composition (wt. %) of K_2O 9.87, Rb_2O 2.86, Cs_2O 0.86, Na_2O 0.26, FeO 0.26, MnO 0.43, Al_2O_3 23.65, SiO_2 52.42, and F 9.35. The Li_2O content analyses yielded an average composition of 3.85 wt % by LA-MC-ICP-MS, resulting in a total of 99.87. The empirical chemical formula calculated on the basis of 10 O^{2-} and 2 F^- a*pfu*. is $(K_{0.85}Rb_{0.12}Cs_{0.02}Na_{0.03})_{\Sigma 1.02}[Li_{1.05}Al_{1.44}(\square_{0.47}Fe_{0.01}Mn_{0.02})_{\Sigma 0.5}]_{\Sigma 2.99}(Si_{3.55}Al_{0.45})_{\Sigma 4}O_{10}F_2$. The ideal formula is $K(LiAl_{1.5}\square_{0.5})(Si_{3.5}Al_{0.5})O_{10}F_2$, which requires K_2O 11.88, Li_2O 3.77, Al_2O_3 25.73, SiO_2 53.07, F 9.59, O≡F −4.04, total 100 wt. %. Compared to polylithionite in the Nanyangshan LCT deposit, fluorluanshiweiite contains more Rb, less Si and more Al. The high fluorine content is a key feature that distinguishes fluorluanshiweiite from luanshiweiite (Table 1).

Table 1. Chemical composition (wt. %) of fluorluanshiweiite and other lepidolite species in nanyangshan LCT deposit.

%	Fluorluanshiweiite			Luanshiweiite			Polylithionite		
	Mean	apfu	σ †	Mean	apfu	σ	Mean	apfu	σ
K_2O	9.87	0.85	0.20	10.58	0.89	0.16	10.88	0.91	0.31
Rb_2O	2.86	0.12	0.09	1.41	0.06	0.07	0.76	0.03	0.15
Cs_2O	0.86	0.02	0.17	0.21	0.01	0.21	0.65	0.02	0.11
Na_2O	0.26	0.03	0.05	0.36	0.05	0.11	0.05	0.01	0.22
Li_2O *	3.85	1.05	0.22	3.85	1.02	0.35	7.70	2.04	0.29
FeO	0.26	0.01	0.10	0.08	0.00	0.23	0.00	0.00	0.00
MnO	0.43	0.02	0.18	0.07	0.00	0.15	0.01	0.00	0.17
Al_2O_3	23.65	1.88	0.57	24.86	1.93	0.65	16.00	1.24	0.45
SiO_2	52.42	3.54	0.64	53.45	3.52	0.56	57.95	3.81	0.59
F	9.35	2.00	0.24	1.31	0.27	0.31	9.71	2.02	0.27
F≡O	−3.93			−0.55			−4.08		
H_2O^+				4.07					
Total	99.88			99.7			99.63		

Notes: * average composition by LA-MC-ICP-MS, others by EPMA. † the standard deviation refers to the weight oxides.

4. Spectroscopic Features

Spectroscopic analyses were performed at the Beijing Research Institute of Uranium Geology. Infrared spectroscopic data of fluorluanshiweiite were obtained using a Bruker LUMOS spectrometer with an ATR model in the range 600–4000 cm^{-1}. Raman spectra were recorded on a LabRAM HR Raman microscope with a laser excitation wavelength of 532 nm. The power of the excitation radiation was 20 mW, and the lateral resolution was estimated to be 1 μm. The results were acquired in the range 100–2000 cm^{-1}.

4.1. Infrared Spectroscopy

The vibrations of mica group minerals can be roughly separated into the vibrational region of hydroxyl groups and the lattice vibrational region, including the vibrations of $Si(Al)O_4$ tetrahedra and octahedrally coordinated cations [13]. In the IR spectrum of fluorluanshiweiite (Figure 2), the bands at 747 and 791 cm^{-1} are due to the Al–O fundamental modes, and the bands at 955, 979, and 1085 cm^{-1} are due to the Si–O fundamental modes, resembling the spectrum of luanshiweiite (760, 798, 891, 988, and 1115 cm^{-1}) [1] and similar to the infrared spectral reference cards (Sil59, Sil60) of the lepidolite series [14].

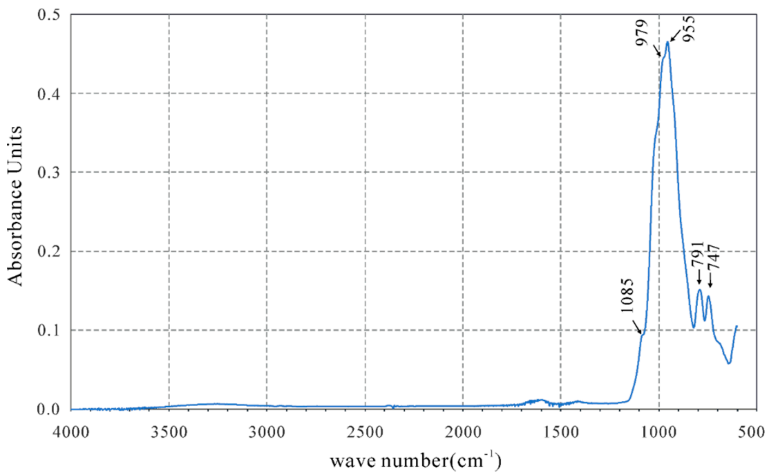

Figure 2. Infrared spectra of fluorluanshiweiite.

There is no evidence for the high-energy OH stretching vibrations that commonly occur in the region from 3750–3550 cm^{-1} for mica group minerals. The defining characteristic of the infrared spectrum is the absence of the high-energy hydroxyl stretching vibration absorption band at −3620 cm^{-1} [1], which is the most significant difference between fluorluanshiweiite and luanshiweiite. The chemical analyses confirm that the *A* site in the new mineral is fully occupied by F (Table 1).

4.2. Raman Spectroscopy

The resulting Raman spectrum of fluorluanshiweiite resembles that of a "Cs-bearing lepidolite" from lepidolite granite, Yichun, China (peaks: 181, 240, 710, and 1141 cm^{-1}) [15], and is similar to the RRUFF Project database spectra of the lepidolite series (X050113, R040101.3, R050132.4). The typical peak for phyllosilicate minerals at ~700 cm^{-1} is well displayed for fluorluanshiweiite (711 cm^{-1}), corresponding to both Si–O stretching and O–Si–O bending deformations. The peaks at approximately 559 and 1139 cm^{-1} are attributed to the stretching mode of the Si–O bond in SiO_4 tetrahedra [16–18].

Raman spectra of mica minerals show several peaks in the low-wavenumber region: ~100, ~160, ~195, ~220, and ~240 cm^{-1}, of which peaks at ~195 and ~240 cm^{-1} are generally strong in diocatahedral lepidolite [19]. On the basis of the previous results of Loh [20], the peaks at 182 and 245 cm^{-1} for fluorluanshiweiite may be assigned to the internal vibrations of the MO_6 octahedron (Figure 3).

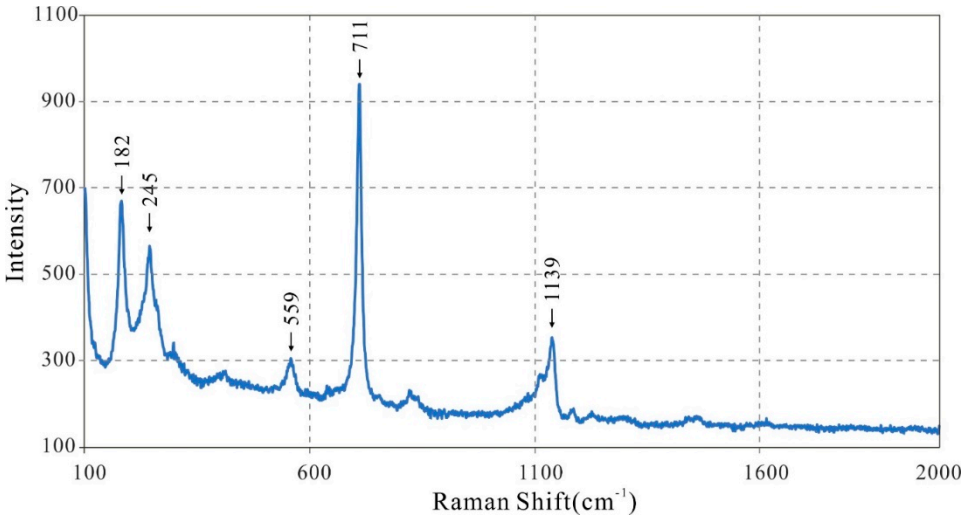

Figure 3. Raman spectra of fluorluanshiweiite.

5. Crystal Structure

Both powder and single-crystal X-ray diffraction data of fluorluanshiweiite were collected on a Rigaku Oxford diffraction XtaLAB PRO-007HF microfocus rotating anode X-ray source (1.2 kW, MoKα, λ = 0.71073 Å) and a hybrid pixel array detector single-crystal diffractometer using Mo$K\alpha$-radiation in the Laboratory of Crystal Structure, China University of Geosciences (Beijing, China).

X-ray powder diffraction data are given in Table 2. The reflection intensities are close to those of the theoretical pattern of lepidolite-1*M* (database ICDD, card no. 85-911). The strongest eight lines in the X-ray diffraction pattern are [*d* in Å(*I*)(hkl)]: 8.427(25) (001), 4.519(57) (020), 4.121(25) (021), 3.628(61) ($\bar{1}$12), 3.350(60) (022), 3.091(46) (112), 2.586(100) ($\bar{1}$30), and 1.506(45) (312). The powder X-ray diffraction data are reported in Table 2.

Table 2. X-ray powder diffraction data (*d* in Å) for fluorluanshiweiite (8 strongest lines are in bold).

I_{meas}	d_{meas}	d_{calc}	*hkl*	I_{meas}	d_{meas}	d_{calc}	*hkl*
25	**8.427**	**9.956**	**001**	9	2.1984	2.1926	041
57	**4.5191**	**4.4956**	**020**	14	2.1414	2.1386	$\bar{1}33$
14	4.3396	4.3242	$\bar{1}11$	3	2.0992	2.0988	221
25	**4.1208**	**4.0975**	**021**	10	1.9959	2.0005	$\bar{2}23$
14	3.8564	3.8368	111	7	1.957	1.9537	133
61	**3.6276**	**3.6154**	$\bar{1}12$	4	1.7209	1.7237	223
60	**3.3495**	**3.3368**	**022**	11	1.6614	1.6612	$\bar{2}42$
46	**3.091**	**3.0802**	**112**	16	1.6403	1.6434	$\bar{1}16$
25	2.8975	2.8904	$\bar{1}13$	10	1.5824	1.5845	$\bar{2}43$
17	2.6795	2.6705	023	6	1.5492	1.5494	$\bar{1}53$
100	**2.5859**	**2.5856**	$\bar{1}30$	**45**	**1.5061**	**1.507**	**312**
25	2.4571	2.466	131	5	1.3821	1.3778	225
25	2.3903	2.3873	$\bar{1}32$	10	1.343	1.343	136
17	2.2539	2.2478	040	21	1.298	1.301	$\bar{3}16$

A colorless flake of fluorluanshiweiite was selected for the single-crystal X-ray diffraction data collection. All reflections were indexed on the basis of a monoclinic unit cell. The structure was solved and refined using *SHELX* Software [21] based on the space group *C*2/*m*. Unit-cell parameters were as follows: a = 5.2030(5), b = 8.9894(6), c = 10.1253(9) Å, β = 100.68(1)° and V = 465.37(7) Å^3. Anisotropic refinement using all measured independent data and reflections with $Fo \geq 4\sigma$ resulted in an R_1 factor of 0.091. The relatively large R_1 could be due to the crystal quality being imperfect; such values for the R factor are relatively often reported for the lepidolite series. In addition, the high R_1 factor of micas may also be affected by the Durovič effect [22]. The crystal structure refinement details for fluorluanshiweiite are reported in Table 3. A view of the structure is presented in Figure 4. Refined coordinates and anisotropic-displacement parameters are presented in Tables 4 and 5, and selected bond lengths and angles are given in Table 6.

Table 3. Crystallographic data and refinement results for fluorluanshiweiite.

Crystal Symmetry	Monoclinic
Space group	*C*2/*m*
Polytype	1*M*
a (Å)	5.2030(5)
b (Å)	8.9894(6)
c (Å)	10.1253(9)
β (°)	100.68(1)
V (Å^3)	465.37(7)
Z	2
Density(cal.) (g/cm^3)	2.898
Radiation type	Mo$K\alpha$
$2\theta_{max}$ (°)	60
total reflections	1255
independent reflections	577
reflections with $Fo \geq 4\sigma$	516
Final R_1	0.091
wR_2 factors	0.202
Goodness-of-fit	1.318
Largest diff. peak and hole (e$^-$/Å^3)	1.203–0.815

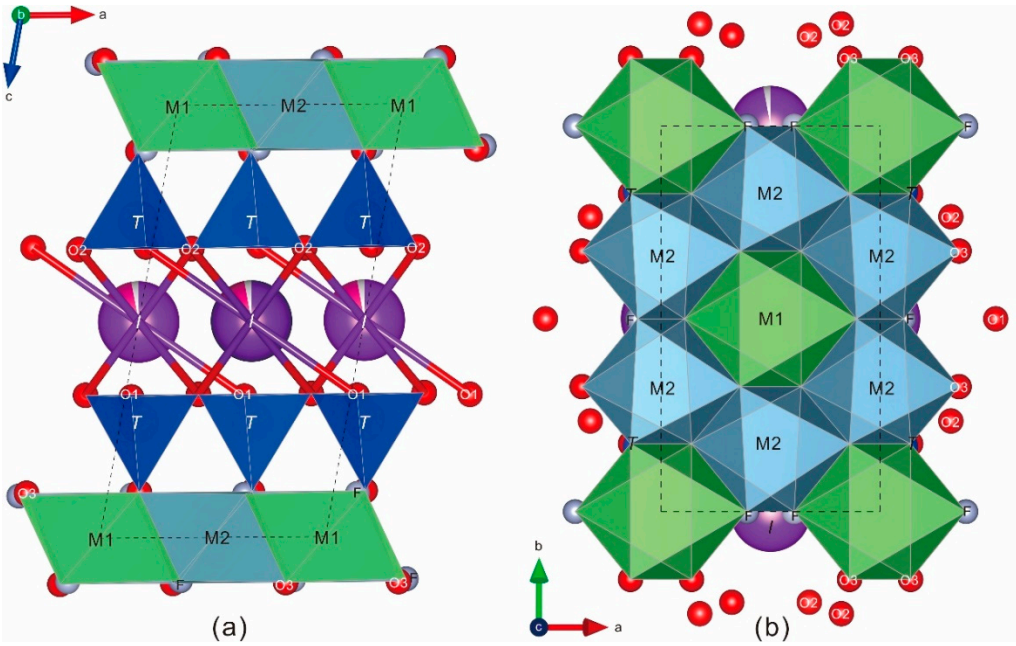

Figure 4. The crystal structure of fluorluanshiweiite: (**a**) view along the *b* axis and (**b**) view along the *c* axis. dark blue: Si tetrahedra(*T*); green: Li octahedra(*M*1); blue-gray: Al octahedra(*M*2); purple: *I*-site.

Table 4. Atomic coordinates and isotropic displacement parameters (in Å^2) for fluorluanshiweiite.

Atom	Wyck.	*s.o.f.*	*x*	*y*	*z*	U_{eq}
K1	2*d*	0.85	0	1/2	1/2	0.0306(9)
Rb1	2*d*	0.12	0	1/2	1/2	0.0306(9)
Li1	2*a*		1/2	1/2	0	0.0160(5)
Al1	4*g*	0.71	1/2	0.8277(5)	0	0.0206(11)
Si1	8*j*	0.88	0.4185(4)	0.6681(2)	0.2673(2)	0.0185(6)
Al2	8*j*	0.12	0.4185(4)	0.6681(2)	0.2673(2)	0.0185(6)
O1	4*i*		0.4722(19)	1/2	0.3264(9)	0.0270(2)
O2	8*j*		0.6769(11)	0.7649(7)	0.3313(6)	0.0258(13)
O3	8*j*		0.3605(11)	0.6759(6)	0.1056(6)	0.0229(13)
F1	4*i*		0.8921(16)	1/2	0.0994(8)	0.0470(2)

Notes: *I* site is fixed by 0.85K + 0.12Rb, *M2* site is fixed by 0.71Al and *T* site is fixed by 0.88Si + 0.12Al.

Table 5. Anisotropic displacement parameters (in Å^2) for fluorluanshiweiite.

Atom	U_{11}	U_{22}	U_{33}	U_{12}	U_{13}	U_{23}
K1	0.0279(18)	0.0253(17)	0.040(2)	0.00000	0.0088(15)	0.00000
Rb1	0.0279(18)	0.0253(17)	0.040(2)	0.00000	0.0088(15)	0.00000
Li1	0.011(11)	0.013(12)	0.028(13)	0.00000	0.013(10)	0.00000
Al1	0.018(2)	0.016(2)	0.029(2)	0.00000	0.0080(19)	0.00000
Si1	0.0147(11)	0.0133(11)	0.0286(11)	−0.0006(7)	0.0067(8)	0.0018(8)
Al2	0.0147(11)	0.0133(11)	0.0286(11)	−0.0006(7)	0.0067(8)	0.0018(8)
O1	0.037(5)	0.012(4)	0.033(5)	0.00000	0.006(4)	0.00000
O2	0.016(3)	0.028(3)	0.035(3)	−0.008(2)	0.009(2)	−0.002(3)
O3	0.022(3)	0.015(3)	0.034(3)	−0.001(2)	0.011(2)	−0.001(2)
F1	0.025(4)	0.088(8)	0.030(4)	0.00000	0.008(3)	0.00000

Table 6. Selected bond lengths (Å) and angles (°) for fluorluanshiweiite.

K1—O1	2.973(9) × 2	Al1—O3	1.955(8) × 2
K1–O1′	3.275(10) × 2	Al1–O3′	1.979(6) × 2
K1–O2	2.969(6) × 4	Al1–F1	1.984(7) × 2
K1–O2′	3.218(6) × 4	<*M*2–O>	1.973
<*I*–O> inner	2.970	Si1–O1	1.631(4)
<*I*–O> outer	3.237	Si1–O2	1.631(8)
Li1–O3	2.112(6) × 4	Si1–O2′	1.632(6)
Li1–F1	2.101(8) × 2	Si1–O3	1.610(6)
<*M1*–O>	2.108	<*T*–O>	1.626
O1^{i}–K1–O2^{i}	49.56(10)	Si1–O1–K1^{ii}	107.25(7)
O2^{i}–K1–O1	94.95(10)	Si1–O1–K1	95.63(7)
F1–Li1–O3	98.74(16)	K1^{ii}–O1–K1	112.58(29)
F1–Li1–O3	81.3(2)	Si1–O2–K1^{ii}	97.19(24)
O3–Si1–O2	111.35(32)	Si1–O3–Al1	124.83(34)
O3–Si1–O1	113.76(23)	Si1–O3–Li1	117.43(32)
O2–Si1–O1	105.99(24)	Al1–O3–Li1	92.79(22)

Symmetry codes: (i) −1 + x, y, z; (ii) 1 + x, y, z.

6. Discussion

The structure of fluorluanshiweiite is similar to that of other species of the mica group. The general formula of mica group minerals may be written as $IM_{2-3}\square_{1-0}T_4O_{10}A_2$ [23]; for fluorluanshiweiite, *I* is K, *M* is Li + 1.5Al + 0.5□, *T* is 3.5Si + 0.5Al, and *A* is 2F. Regarding the interlayer cation, the difference between the inner (mean 2.970 Å) and outer (mean 3.237 Å) <*I*–O> distances is similar to that in the luanshiweiite-2M_1 structure (2.938 and 3.251 Å, respectively). The mean <*M*1–O> distance in fluorluanshiweiite is 2.108 Å, including the Li–O distance, 2.112 Å, and the Li-F distance, 2.101 Å. These distances are comparable to the sum of the ionic radii of Li^+, O^{2-} and F^- (0.76, 1.40 and 1.38 Å, respectively) [24] and are slightly shorter than the luanshiweiite Li–O distance, 2.140 Å. The <*M*2–O> distance (mean 1.973 Å) is similar to that of luanshiweiite (mean 1.957 Å) and longer than the values given by Shannon and Prewitt [25] for Al–O (1.91 Å). The octahedral distance from the center of a vacant site to the nearest six oxygen atoms should be considered in reference to other mica minerals, e.g., montdorite and yangzhumingite [26–29]. In this case, the occurrence of 0.5 vacancies at the *M*2 site in fluorluanshiweiite must be considered. On the basis of the mean □–O distance in reported dioctahedral micas of 2.174 Å [30,31], the ideal <*M*2–O> distance in fluorluanshiweiite should be 1.976 Å, which is similar to the distance 1.973 Å observed. The mean <*T*–O> distance (1.626 Å) in fluorluanshiweiite is similar to that in luanshiweiite (mean 1.628 Å), longer than that in polylithionite (1.621 Å) [32] and shorter than that in trilithionite (1.638 Å) [33,34] due to substitution of smaller Si^{4+} and larger Al^{3+} in the tetrahedral layer, which is consistent with the occupancy of Si and Al at the *T* site in the lepidolite species above. Octahedral vacancies can be introduced by a substitution mechanism such as $Li^+ + 0.5Si^{4+} \leftrightarrow Al^{3+} + 0.5\square$.

Bond-valence analysis (BVS): The bond valence (*vu*) was calculated from the interatomic distance following the procedure of Brown and Altermatt [35]. The bond-valence sums for the *I*(K), *M1*(Li), *M2*($Al_{1.5}\square_{0.5}$), and *T*($Si_{3.5}Al_{0.5}$) positions are 0.95, 0.97, 2.31, and 3.97 valence units (*vu*), respectively, which is in agreement with the expected values given that various cations are present at the same sites. The low BVS for *M*2 suggests that it has a vacant cation position. The bond-valence sums for the O1, O2, and O3 positions are 2.11, 2.12, and 2.06 *vu*, respectively. The bond-valence sum for the *A* site, which is occupied by a hydroxyl group in luanshiweiite [1], is 0.89 *vu* for F in fluorluanshiweiite. As shown in Table 7, all the resulting BVS values are comparable to ideal values, and the model basically matches the charge balance requirement.

In conclusion, fluorluanshiweiite is the third light mica with substantial lithium and a stoichiometry intermediate between diocatahedral and trioctahedral; only two other Li micas have this stoichiometry:

luanshiweiite [1] and voloshinite [2]. Fluorluanshiweiite can be considered as the F-dominant analogue at the *A* site of luanshiweiite or a K-dominant analogue at the *I* site of voloshinite (Table 8).

Table 7. Bond-valence (vu) analysis for fluorluanshiweiite.

	***I*-site**	***M*1-site**	***M*2-site**	***T*-site**	**Sum**
O1	0.105 × 2↓			0.980 × 2→	2.11
	0.046 × 2↓				
O2	0.107 × 4↓			0.980	2.12
	0.054 × 4↓			0.977	
O3		0.175 × 4↓	0.440 × 2↓	1.037	2.06
			0.412 × 2↓		
F1		0.135 × 2↓→	0.308 × 2↓→		0.89
Sum	0.95	0.97	2.31	3.97	

Notes: Bond valence sums were calculated with the site-occupancy factors given in Table 4. Calculations were done using the equation and constants of [36], $S = \exp[(R_0–d_0)/b]$. The symbols → and ↓ mean that the value must be multiplied by a factor 2 or 4 horizontally and vertically, respectively.

Table 8. Comparative characteristics of fluorluanshiweiite and other minerals of the lepidolite species having a similar structure.

	Fluorluanshiweiite			**Luanshiweiite ***			**Voloshinite †**		
I-site	K			K			Rb		
M-site	$LiAl_{1.5}\square_{0.5}$			$LiAl_{1.5}\square_{0.5}$			$LiAl_{1.5}\square_{0.5}$		
T-site	$Si_{3.5}Al_{0.5}$			$Si_{3.5}Al_{0.5}$			$Si_{3.5}Al_{0.5}$		
A-site	F_2			$(OH)_2$			F_2		
Crystal system	Monoclinic			Monoclinic			Monoclinic		
Space group	*C*/2*m*			*C*2/*c*			*C*2/*c*		
Polytype	1*M*			$2M_1$			$2M_1$		
a(Å)	5.2030(5)			5.1861(7)			5.191		
b(Å)	8.9894(6)			8.9857 (13)			9.025		
c(Å)	10.1253(9)			19.970(3)			20.40		
β(°)	100.68(1)			95.420(3)			95.37		
V(Å^3)	465.37(7)			926.5(2)			951.5		
Z	2			4			4		
Density(cal.)	2.898			2.868			2.95		
Optical properties	biaxial (–)			biaxial (–)			biaxial (–)		
α	1.554			1.5474			1.511		
β	1.581			1.5700			1.586		
γ	1.583			1.5729			1.590		
2*V*(cal.)	30°			39°			25°		
	d_{meas}	I_{meas}	*hkl*	d_{meas}	I_{meas}	*hkl*	d_{meas}	I_{meas}	*hkl*
Selected strongest lines in the powder pattern, The intensities of 8 strongest lines are in bold.	**8.427**	**25**	**001**	**9.891**	**35**	**002**	**10.100**	**60**	**002**
	4.519	**57**	**020**	**4.451**	**31**	**$\bar{1}$11**	**4.550**	**80**	**020**
	3.856	14	111	3.870	11	$\bar{1}$13	3.980	40	112
	3.628	**61**	**$\bar{1}$12**	**3.703**	**12**	**023**	**3.770**	**40**	**023**
	3.350	**60**	**022**	**3.314**	**36**	**006**	**3.350**	**60**	**006**
	3.091	**46**	**112**	**3.090**	**40**	**$\bar{1}$15**	**3.220**	**40**	**114**
	2.898	25	$\bar{1}$13	2.973	34	025	3.020	45	025
	2.680	17	023	2.769	24	$\bar{1}$16	2.805	30	$\bar{1}$16
	2.586	**100**	**$\bar{1}$30**	**2.565**	**100**	**116**	**2.575**	**100**	**116**
	2.457	25	131	2.454	12	$\bar{1}$33	2.469	15	$\bar{1}$33
	2.390	**25**	**$\bar{1}$32**	**2.378**	**31**	**133**	**2.410**	**20**	**133**
	2.254	17	$\bar{2}$21	2.243	11	$\bar{2}$21	2.234	10	$\bar{2}$22
	2.141	14	$\bar{1}$33	2.130	27	043	2.141	40	135
	1.996	10	$\bar{2}$23	1.986	30	00,10	1.986	10	224
	1.640	16	$\bar{1}$16	1.647	32	$\bar{3}$14	1.660	30	$\bar{3}$14
	1.506	**45**	**312**	**1.500**	**26**	**060**	**1.501**	**40**	**$\bar{3}$32**
	1.343	10	$\bar{3}$16	1.345	14	$\bar{1}$3,13	1.351	10	$\bar{1}$3,13

Notes: Data reference from * Reference [1], † Reference [2].

Author Contributions: K.Q., X.S., G.L., G.F., and G.S. designed the experiments and wrote the paper; G.L. collected the single-crystal X-ray diffraction data and analyzed the crystal structure data; L.Q. obtained the IR spectra and analyzed IR and Raman data; Y.W., X.L., and Z.X. obtained the lithium content data; and G.F. and H.G. collected the electron-microprobe data. All authors have read and agreed to the published version of the manuscript.

Funding: Financial support for this research was received from the Natural Science Foundation of China (NSFC Grant 41502033) and the China Geological Survey Project (DD20160129-3, DD20190813, 1212011120771).

Acknowledgments: The authors acknowledge Ritsuro Miyawaki, Chairman of the IMA-CNMNC, and the members of the IMA-CNMNC for their helpful comments on the data submitted for the new mineral proposal. The reviewers and editor are acknowledged for their constructive comments.

Conflicts of Interest: The authors declare no conflicts of interest.

References

1. Fan, G.; Li, G.; Shen, G.; Xu, J.; Dai, J. Luanshiweiite: A New Member of Lepidolite Series. *Acta Mineral. Sin.* **2013**, *33*, 713–721. (In Chinese with English abstract)
2. Pekov, I.V.; Kononkova, N.N.; Agakhanov, A.A.; Belakovsky, D.I.; Kazantsev, S.S.; Zubkova, N.V. Voloshinite, a new rubidium mica from granitic pegmatite of Voron'i Tundras, Kola Peninsula, Russia. *Geol. Ore Depos.* **2010**, *52*, 591–598. [CrossRef]
3. Qu, K.; Sima, X.; Li, G.; Fan, G.; Shen, G.; Liu, X.; Xiao, Z.; Hu, G.; Qiu, L.; Wang, Y. Fluorluanshiweiite, IMA 2019-053. CNMNC Newsletter No. 52. *Mineral. Mag.* **2019**, *83*, 887–893.
4. Luan, S.; Mao, Y.; Fan, L.; Wu, X.; Lin, J. *Mineralization and Prospection of Rare Earth Metals in the Koktogay Area*; Chengdu University of Science and Technology Press: Chengdu, China, 1995; pp. 66–194. (In Chinese)
5. Černý, P. Rare-element granitic pegmatites. I. Anatomy and internal evolution of pegmatite deposits. *Geosci. Can.* **1991**, *18*, 49–67.
6. Černý, P.A.; Ercit, T.S. The classification of granitic pegmatites revisited. *Can. Mineral.* **2005**, *43*, 2005–2026. [CrossRef]
7. 9th Laboratory of Chengdu Institute of Geology. The isotopic dating of geological ages of granites and pegmatites in the eastern part of the Eastern Tsinling. *Geochimica* **1973**, *3*, 166–172. (In Chinese with English abstract)
8. Qu, K.; Sima, X.Z.; Zhou, H.Y.; Xiao, Z.B.; Tu, J.R.; Yin, Q.Q.; Liu, X.; Li, J.H. In situ LA-MC-ICP-MS and ID-TIMS U-Pb ages of bastnäsite-(Ce) and zircon from the Taipingzhen hydrothermal REE deposit: New constraints on the Later Palaeozoic granite-related U-REE mineralization in the North Qinling Orogen, Central China. *J. Asian Earth Sci.* **2019**, *173*, 352–363. [CrossRef]
9. Guo, J.J.; Li, H.K.; Chen, Z.H. Brief Review of the Study of Qinling Complex, Qinling Orogenic Belt. *Geol. Surv. Res.* **2003**, *26*, 95–102. (In Chinese with English abstract)
10. Geng, J.Z.; Huang, Y.Q.; Jian, G.P.; Wu, L.; Zhu, R.; Yu, H.C.; Qiu, K.F. Zircon U-Pb age and Lu-Hf isotopes of the dacite from Zaozigou Au-Sb deposit, west Qinling, China. *Geol. Surv. Res.* **2019**, *42*, 166–173. (In Chinese with English abstract)
11. Fan, G.; Ge, X.; Li, G.; Yu, A.; Shen, G. Oxynatromicrolite, $(Na,Ca,U)_2Ta_2O_6(O,F)$, a new member of the pyrochlore supergroup from Guanpo, Henan Province, China. *Mineral. Mag.* **2017**, *81*, 743–751.
12. Mandarino, J.A. The Gladstone-dale relationship: Part The compatibility concept and its application. *Can. Mineral.* **1981**, *19*, 441–450.
13. Beran, A. Infrared spectroscopy of micas. *Rev. Mineral. Geochem.* **2002**, *46*, 351–369. [CrossRef]
14. Chukanov, N.V. *Infrared Spectra of Mineral Species: Extended Library*; Springer Science & Business Media: Dordrecht, The Netherlands, 2013; p. 459.
15. Wang, R.C.; Hu, H.; Zhang, A.C.; Huang, X.L.; Ni, P. Pollucite and the caesium-dominant analogue of polylithionite as expressions of extreme Cs enrichment in the Yichun topaz–lepidolite granite, southern China. *Can. Mineral.* **2004**, *42*, 883–896. [CrossRef]
16. McKeown, D.A.; Bell, M.I.; Etz, E.S. Raman spectra and vibrational analysis of the trioctahedral mica phlogopite. *Am. Mineral.* **1999**, *84*, 970–976. [CrossRef]
17. McKeown, D.A.; Bell, M.I.; Etz, E.S. Vibrational analysis of the dioctahedral mica: $2M_1$ muscovite. *Am. Mineral.* **1999**, *84*, 1041–1048. [CrossRef]

18. Wang, A.L.; Freeman, J.; Kuebler, K.E. Raman Spectroscopic Characterization of Phyllosilicates. In *Lunar and Planetary Science XXXIII*; Document ID: 20020045549; NASA Goddard Space Flight Center: Greenbelt, MD, USA, 2002.
19. Tlili, A.; Smith, D.C.; Beny, J.M.; Boyer, H. A Raman microprobe study of natural micas. *Mineral. Mag.* **1989**, *53*, 165–179. [CrossRef]
20. Loh, E. Optical vibrations in sheet silicates. *J. Phys. C Solid State Phys.* **1973**, *6*, 1091. [CrossRef]
21. Sheldrick, G.M. Crystal structure refinement with SHELXL. *Acta Crystallogr. C* **2015**, *71*, 3–8. [CrossRef]
22. Nespolo, M.; Ferraris, G. Effects of the stacking faults on the calculated electron density of mica polytypes—The Durovic effect. *Eur. J. Mineral.* **2001**, *13*, 1035–1045. [CrossRef]
23. Rieder, M.; Cavazzini, G.; D'yakonov, Y.D.; Frank-Kamenetskii, V.A.; Gottardi, G.; Guggenheim, S.; Müller, G.; Neiva, A.M.R.; Radoslovich, E.W.; Robert, J.L.; et al. Nomenclature of the micas. *Can. Mineral.* **1998**, *36*, 905–912. [CrossRef]
24. Shannon, R.D. Revised effective ionic radii and systematic studies of interatomic distances in halides and chalcogenides. *Acta Cryst. A* **1976**, *32*, 751–767. [CrossRef]
25. Shannon, R.T.; Prewitt, C.T. Effective ionic radii in oxides and fluorides. *Acta Cryst. B* **1969**, *25*, 925–946. [CrossRef]
26. Toraya, H.; Iwai, S.; Makimo, F.; Kondo, R.; Daimon, M. The crystal structure of tetrasilicic potassium fluor mica, $KMg_{2.5}Si_4O_{10}F_2$. *Z. Krist.* **1976**, *144*, 42–52. [CrossRef]
27. Robert, J.L.; Maury, R.C. Natural occurrence of a (Fe, Mn, Mg) tetrasilicic potassium mica. *Contrib. Mineral. Petrol.* **1979**, *68*, 117–123. [CrossRef]
28. Miyawaki, R.; Shimazaki, H.; Shigeoka, M.; Yokoyama, K.; Matsubara, S.; Yurimoto, H. Yangzhumingite, $KMg_{2.5}Si_4O_{10}F_2$, a new mineral in the mica group from Bayan Obo, Inner Mongolia, China. *Eur. J. Mineral.* **2011**, *23*, 467–473. [CrossRef]
29. Schingaro, E.; Kullerud, K.; Lacalamita, M.; Mesto, E.; Scordari, F.; Zozulya, D.; Ermabert, M.; Ravna, E.J. Yangzhumingite and phlogopite from the Kvaløya lamproite (North Norway): Structure, composition and origin. *Lithos* **2014**, *210*, 1–13. [CrossRef]
30. Brigatti, M.F.; Kile, D.E.; Poppi, M. Crystal structure and crystal chemistry of lithium-bearing muscovite-2M_1. *Can. Mineral.* **2001**, *39*, 1171–1180. [CrossRef]
31. Drits, V.A.; Zviagina, B.B.; McCarty, D.K.; Salyn, A.L. Factors responsible for crystal-chemical variations in the solid solutions from illite to aluminoceladonite and from glauconite to celadonite. *Am. Mineral.* **2010**, *95*, 348–361. [CrossRef]
32. Hawthorne, F.C.; Sokolova, E.; Agakhanov, A.A.; Pautov, L.A.; Karpenko, V.Y. The Crystal Structure of Polylithionite-1*M* from Darai-pioz, Tajikistan: The Role of Short-Range Order in Driving Symmetry Reduction in 1*M* Li-Rich Mica. *Can. Mineral.* **2019**, *57*, 519–528. [CrossRef]
33. Brigatti, M.F.; Caprilli, E.; Malferrari, D.; Medici, L.; Poppi, L. Crystal structure and chemistry of trilithionite-2M_2 and polylithionite-2M_2. *Eur. J. Mineral.* **2005**, *17*, 475–481. [CrossRef]
34. Brigatti, M.F.; Mottana, A.; Malferrari, D.; Cibin, G. Crystal structure and chemical composition of Li-, Fe-, and Mn-rich micas. *Am. Mineral.* **2007**, *92*, 1395–1400. [CrossRef]
35. Brown, I.D.; Altermatt, D. Bond-valence parameters obtained from a systematic analysis of the Inorganic Crystal Structure Database. *Acta Crystallogr. Sect. B* **1985**, *41*, 244–247. [CrossRef]
36. Brown, I.D. Predicting bond lengths in inorganic crystals. *Acta Crystallogr. B* **1977**, *33*, 1305–1310. [CrossRef]